HHS Public Access

Author manuscript

J Biomed Mater Res A. Author manuscript; available in PMC 2020 January 30.

Published in final edited form as:

J Biomed Mater Res A. 2018 April ; 106(4): 1104–1110. doi:10.1002/jbm.a.36310.

3D printed hyperelastic "bone" scaffolds and regional gene therapy: A novel approach to bone healing

Ram Alluri[1], **Adam Jakus**[2,3,4], **Sofia Bougioukli**[1], **William Pannell**[1], **Osamu Sugiyama**[1], **Amy Tang**[1], **Ramille Shah**[3,4,5,6], **Jay R. Lieberman**[1]

[1]Department of Orthopaedic Surgery, Keck School of Medicine of the University of Southern California, 2011 Zonal Ave, HMR 702, Los Angeles, California 90089

[2]Department of Materials Science and Engineering, Northwestern University, 303 E. Superior St., 11th Floor, Chicago, Illinois 60611

[3]Department of Materials Science and Engineering, Northwestern University, 2220 Campus Dr., Evanston, IL 60208

[4]Simpson Querrey Institute for BioNanotechnology, Northwestern University, 303 E Superior St., Chicago, IL 60611

[5]Department of Biomedical Engineering, Northwestern University, 2145 Sheridan Rd., Evanston, IL 60208

[6]Department of Surgery, Division of Organ Transplantation, Northwestern University, 251 E Huron St., Chicago, IL 60611

Abstract

The purpose of this study was to evaluate the viability of human adipose-derived stem cells (ADSCs) transduced with a lentiviral (LV) vector to overexpress bone morphogenetic protein-2 (BMP-2) loaded onto a novel 3D printed scaffold. Human ADSCs were transduced with a LV vector carrying the cDNA for BMP-2. The transduced cells were loaded onto a 3D printed Hyperelastic "Bone" (HB) scaffold. *In vitro* BMP-2 production was assessed using enzyme-linked immunosorbent assay analysis. The ability of ADSCs loaded on the HB scaffold to induce *in vivo* bone formation in a hind limb muscle pouch model was assessed in the following groups: ADSCs transduced with LV-BMP-2, LV-green fluorescent protein, ADSCs alone, and empty HB scaffolds. Bone formation was assessed using radiographs, histology and histomorphometry. Transduced ADSCs BMP-2 production on the HB scaffold at 24 hours was similar on 3D printed HB scaffolds versus control wells with transduced cells alone, and continued to increase after 1 and 2 weeks of culture. Bone formation was noted in LV-BMP-2 animals on plain radiographs at 2 and 4 weeks after implantation; no bone formation was noted in the other groups. Histology demonstrated that the LV-BMP-2 group was the only group that formed woven bone and the mean bone area/tissue area was significantly greater when compared with the other groups. 3D printed HB scaffolds are effective carriers for transduced ADSCs to promote bone repair. The combination of gene therapy

Correspondence to: J. R. Lieberman; Jay.Lieberman@med.usc.edu.

Additional Supporting Information may be found in the online version of this article.

and tissue engineered scaffolds is a promising multi-disciplinary approach to bone repair with significant clinical potential.

Keywords

3D printing; gene therapy; bone; tissue engineering; scaffold

INTRODUCTION

Significant bone loss is a common complication seen in orthopedic trauma, revision joint arthroplasty, tumor resection, and spinal pseudarthrosis. It is among the most challenging clinical problems that orthopedic surgeons are faced with, and it can result in substantial patient morbidity, consumption of medical resources, and socioeconomic cost.[1] Over 500,000 bone graft procedures are performed annually in the United States.[2] Autologous bone graft remains the gold standard for these difficult to treat bone loss scenarios as it provides an osteoinductive stimulus, osteogenic cells and an osteoconductive scaffold. However, autologous bone grafting is associated with considerable disadvantages including limited quantity, postoperative pain, fractures at the harvest site, nerve damage, and donor site infection.[3–5] Furthermore, bone graft may have limited biologic activity in settings of poor bone stock, systemic illness, compromised vascularity, poor soft tissue coverage, or prior infection.[6] Due to these limitations, there is significant interest in developing bone graft substitutes that have sufficient biologic activity to induce osteogenesis while being efficiently and easily implantable into large, irregular bone defects.

Recombinant human Bone Morphogenetic Protein-2 (rhBMP-2) is one of the most potent growth factors for bone formation and its combination with a scaffold was initially thought to be the optimal clinical solution for bone regeneration; however, the clinical results have been inconsistent. RhBMP-2 is traditionally loaded on to a collagen sponge and it has been hypothesized that the rapid release of the Bone Morphogenetic Protein (BMP) from the sponge limits its osteoinductive activity.[7–9] In order to overcome this limitation, high doses of rhBMP-2 are used clinically which has been associated with reports of postoperative complications including heterotopic bone formation, soft tissue swelling and osteolysis.[10,11]

3D printed scaffolds represent a promising approach for bone repair. 3D printed scaffolds can be customized to fit complex anatomic skeletal defects.[12] More importantly, some 3D printing processes allow for precise control of biologic and biomechanical properties of the scaffold through variations in mineral composition and structure.[13] The ideal scaffold should be non-toxic, biocompatible, possess adequate mechanical properties to withstand shear and axial force, and has porosity that favors bone ingrowth and vascularization. However, most scaffolding materials may not lead to a significant bone healing response, and combination with an osteoinductive stimulus may be required for optimal regeneration.

Several recent studies have evaluated the bone forming potential of 3D printed scaffolds when combined with various osteoinductive stimuli.[14–18] Wang et al.[14] evaluated the osteogenic effect of controlled release rhBMP-2 in 3D printed hydroxyapatite scaffolds. Similarly, Shim et al. used rhBMP-2, but in combination with 3D printed polycaprolactone

(PCL)/poly(lactic-coglycolic acid) (PLGA) scaffolds.[18] Two other studies used 3D printed scaffolds made of PCL or Polyetheretherketone (PEEK) in combination with adipose-derived stem cells (ADSCs).[15,16] Temple et al.[15] loaded ADSCs on a 3D printed PCL scaffold and demonstrated vascularization of the scaffold but no definitive bone formation. Roskies et al.[16] seeded a 3D printed PEEK scaffold with ADSCs and were able to demonstrate osteodifferentiation of the ADSCs as measured by alkaline phosphatase activity during *In vitro* testing; no *in vivo* models were used in this study.

An alternative strategy to the use of rhBMP-2 is the development of regional gene therapy using transduced cells to deliver the BMP-2 protein. This allows for the delivery of both osteoprogenitor cells and an osteoinductive growth factor to a specific anatomic site where the transduced cells can induce bone formation. To-date, no study has evaluated the osteogenic potential of 3D printed scaffolds combined with a prolonged osteoinductive signal using lentiviral (LV) gene therapy. *Ex vivo* regional gene therapy allows for the incorporation of a desired gene (encoding the growth factor essential for bone formation) into host cells and the implantation of these cells back into the host at a specific anatomic site.[19] These transduced cells provide sustained release of the osteoinductive BMP-2 protein that results in new bone formation. Both *in vivo* and *ex vivo* gene therapy strategies have demonstrated successful healing of critical-sized defects in animal models.[19–21] The transduced cells need to be delivered on some type of scaffold or carrier to the specific bone defect site. The type of cell carrier used in regional gene therapy for bone repair has received limited attention and it is our hypothesis that the cell carrier could play a critical role in the bone repair process.

The combination of regional gene therapy and 3D printed scaffolds represents a promising translational approach for bone repair. The purpose of this study was to evaluate the viability of human ADSCs transduced with a LV vector to overexpress BMP-2. The transduced cells were loaded on to a 3D printed scaffold comprised of Hyperelastic “Bone” (HB),[22,23] a novel, surgically friendly composite material containing 90 wt % hydroxyapatite yet is mechanically elastic.

METHODS

Fabrication of 3D printed HB scaffolds

HB 3D-printable inks were synthesized according to previously described methods.[22–27] In brief, polylactic-co-glycolic acid (82:18; PLGA; Evonik; 10% solids by weight) micron-scale hydroxyapatite powder (HA; Sigma; 90% by solids weight), and three solvents: dichloromethane (DCM; Sigma), 2-butoxyathanol (Sigma), and dibutyl phthalate (Sigma) were thoroughly mixed. The resulting mixture was sonicated in a chemical hood, while open, and occasionally stirred, permitting excess DCM to evaporate and the ink to thicken to a viscosity of 30–35 Pa·s. All 3D-printed HB structures were fabricated using a 3D-Bioplotter (EnvisionTEC). The HB ink was 3D-printed into two distinct types of structures; large, 5-cm diameter, 1-mm thick disks for *In vitro* studies, and curved, hollow-cored sleeves based on rat femoral microCT data. All objects were 3D-printed under ambient conditions via direct syringe extrusion using a 250 μm-diameter nozzle at 15–40 mm/s linear deposition speeds (Video 1). Each 5 cm-diameter disk was comprised of eight layers, with 125 μm layer

thickness, and an alternating 0–908 pattern, with every other layer-offset in X and Y at a distance of half the designated in-plane strut spacing (700 μm), similar to previously reported by Jakus et al.[22,23,27] The hollow-cored femoral sleeves were comprised of approximately 50 125 μm-thick layers, with the exterior wall measuring approximately 1 mm in thickness. The walls of the hollow-cored femoral sleeves were printed using an alternating 0–90° pattern with 300 μm strut spacing. The resulting 5-cm diameter cylinders and hollow-cored femoral sleeves were washed in 70% ethanol and sterile, deionized water to remove residual solvents as well as sterilize the material prior to cell seeding.[22–24,26,27]

ADSC isolation and transduction

After approval from the Institutional Review Board, adipose tissue was obtained from healthy donors undergoing elective abdominal, buttock and/or thigh liposuction. The harvested lipoaspirate was washed with phosphate buffered saline and digested with collagenase to obtain the stromal vascular fraction (SVF) as previously described.[28] The resultant cell pellet (SVF) was then maintained in fresh medium consisting of Dulbecco modified Eagle medium (DMEM) (Gibco BRL, Grand Island, New York), 10% fetal bovine serum (FBS), 1% penicillin/streptomycin, and 1% amphotericin-B solution. The cells were filtered, plated at a concentration of 5×10^6 cells per 10 cm plate, and incubated in a humidified atmosphere of 5% CO_2 at 37°C. Culture medium was changed every 3 days, and all nonadherent cells were aspirated from the plates. During each passage, confluent cells were trypsinized, split, and plated with $8–9 \times 10^5$ cells per plate.

A LV with the murine leukemia virus promoter encoding either the BMP-2 (LV-BMP-2) or enhanced green fluorescent protein (LV-GFP) coding sequence was prepared as previously described.[29] Passage three ADSCs were plated in 10-cm dishes at a density of 1×10^6 cells in 5 mL of transduction media per dish. Transduction with the LV was carried out in the presence of 8 mg/mL polybrene at a multiplicity of infection (MOI) of 25 for both LV-BMP-2 and LV-GFP. Cells were then washed and incubated in fresh DMEM + 10% FBS for 24 h. The transduced ADSCs were then harvested for *In vitro* and *in vivo* experiments.

In vitro BMP-2 assay

In vitro BMP-2 production of ADSC/LV-BMP2 loaded on 15-mm 3D printed HB discs (cut from 5 cm discs) was assessed at 24 h, 7, and 14 days of cell culture after transduction. Wells without 3D printed discs (cells alone) were loaded with ADSC/LV-BMP-2 or nontransduced ADSCs to serve as control groups and BMP-2 production was assessed at the same time points. All *In vitro* tests were performed in triplicate and BMP-2 production was assessed by an enzyme-linked immunosorbent assay (ELISA) kit (Quantikine, R&D Systems, Minneapolis, MN) based on manufacturer instructions. Briefly, 400,000 ADSCs were loaded onto the 15-mm 3D printed HB disc or an empty control well at a density of 10,000 cells/microliter of FBS. After incubation for 24 h, 7, or 14 days, the culture medium was harvested for ELISA analysis. The cells were also harvested to allow for cell count calculation and standardization of BMP-2 production per cell number. BMP-2 produced was reported as ng BMP-2/24 h/1×10^6 cells.

Implantation of BMP-2 transduced ADSC on an HB scaffold into NSG mice

Animal care and procedures were performed in accordance with the Institutional Animal Care and Use Committee guidelines after approval of the study protocol. NIH guidelines for the care and use of laboratory animals (NIH Publication no. 85–23 Rev. 1985) were observed. Severe combined immunodeficiency gamma mice (NSG, Cannon lab, Keck School of Medicine, University of Southern California) were used in this study. Animals were anesthetized using inhalational anesthesia (2% isoflurane and oxygen) and the left hind limb was sterilely prepared for the operation. A 2-cm incision was made along the posterolateral aspect of the left thigh and the quadriceps muscle was identified and split. A 6-mm 3D printed HB scaffold (Fig. 1) was implanted into the created muscle pouch. The skin and muscle incision were closed with 5–0 vicryl suture and the animals were allowed *ad libitum* activity. There were four different study groups (groups I–IV) for the animal experiment, each containing five mice (Table I). There was no incubation period as the ADSCs were loaded onto the HB scaffold immediately prior to implantation into the muscle pouch.

Evaluation of bone formation

Radiographic evaluation was performed at 2 and 4 weeks after muscle pouch implantation. All mice were euthanized at 4 weeks post-implantation and the hind limb muscle pouch containing the HB scaffold was harvested and fixed in 10% formalin. Each muscle pouch was decalcified with 10% EDTA and then dehydrated and embedded in paraffin. The embedded tissues were cut into 5-μm sections and histological analysis was performed using hematoxylin-eosin and Masson's trichrome (MT) staining. Following staining, each muscle pouch was imaged using a Nikon AZ100 Multi-zoom microscope (Nikon Instruments Inc, Melville, NY) and analyzed with Bioquant analysis software (Bioquant Image Analysis, Nashville, TN). Briefly, four corners of the muscle pouch on 1.5× magnification images were connected by a line marking the region of interest (ROI). The surface area of the ROI represented the total tissue area (TA). Mature bone in the muscle pouch was identified using a BioQuant threshold tool and the bone surface area (BA) was measured. BA/TA of each muscle pouch from all four groups was then calculated.

Statistical analysis

Statistical analysis was done with SPSS Statistics 22, with the significance level set at 0.05. Data are expressed as mean and SD. After confirming the normality of the data, statistical comparisons were made using independent samples *t* test for BMP-2 production and one-way ANOVA with *post-hoc* analysis with Tukey's range test for histomorphometry (BA/TA).

RESULTS

In vitro assessment

Enzyme-linked immunosorbent assay.—ELISA analysis at 24 h, 7, and 14 days confirmed successful BMP-2 production by the ADSCs transduced with LV-BMP-2 loaded on 3D printed HB scaffolds. After 24 h in culture, ADSC BMP-2 production was similar on

3D printed HB scaffolds (21.1 ± 2.3 ng BMP-2 per 1×10^6 cells) versus control wells (20.4 ± 0.6 ng BMP-2 per 1×10^6 cells) ($p = 0.651$). After 7 and 14 days, transduced ADSCs continued to produce BMP-2 on the HB scaffold, but at levels significantly lower than the control wells ($p < .001$) (Table II).

In vivo assessment

Radiography.—Robust ectopic bone formation was noted at 2 and 4 weeks in all five mice implanted with ADSC/LV-BMP-2 loaded on the HB scaffold (group I) (Fig. 2). No ectopic bone formation was noted in the negative control groups (groups II–IV) (Fig. 2).

Histology.—In the HB scaffold loaded with ADSC/LV-BMP-2, woven bone formation was noted at the interface of the 3D printed HB scaffold and the surrounding muscle pouch 4 weeks after implantation (Fig. 3). There was no evidence of bone formation in the negative control groups (groups II–IV (Fig. 3). Healthy scaffold integration with the surrounding host tissue and extra cellular matrix infiltrating/penetrating the HB material at the scaffold-muscle interface was noted in all four groups. All groups also had tissue integration into the HB scaffold via the large channels on both ends of the scaffold.

Histomorphometric analysis.—Quantitative histomorphometric analysis of the MT stained slides at the 4-week time point confirmed significant differences in bone formation demonstrated by radiographs and qualitative histologic analyses. Mean BA/TA was 0.074 ± 0.03 for the ADSC/LV-BMP-2 group loaded on the HB scaffold group. The BA/TA was significantly greater for the ADSC/LV-BMP-2 group compared between groups II–IV ($p = 0.002$) (Fig. 4).

DISCUSSION

Fracture nonunions, revision total joint arthroplasties and spine pseudoarthrosis remain among the most difficult bone repair scenarios in orthopedic surgery, leading to significant morbidity and increased health care costs. Due to limitations of current treatment options, there is a substantial need for efficacious and efficient alternative treatment strategies to consistently heal large bone defects. In this study we hypothesized that the combination of a precisely designed 3D printed scaffold and transduced mesenchymal stem cells providing an osteoinductive stimulus would promote bone repair, thus providing proof of concept for the development of a new clinical regimen.

3D printed scaffolds, made of different materials, have been previously investigated for use in bone regeneration applications. Though highly osteoconductive, the majority of the scaffolds alone are not thought to be particularly osteoinductive, which limits their applicability in the reconstruction of large bone defects.[30,31] Therefore, recent studies have investigated the combination of 3D printed scaffolds with an added osteoinductive agent such as rhBMP-2.[14,15,18,32,33]

RhBMP-2 is the most potent osteoinductive agent available today; however, rhBMP-2 has not fulfilled its clinical promise. First, when loaded on a collagen sponge, large doses of protein are needed to have an adequate biologic,[8,34] and the use of supraphysiologic doses of

rhBMP-2 has led to questions about its clinical safety, and some clinical studies have demonstrated complications such as soft tissue edema, heterotopic ossification, and cyst formation associated with rhBMP-2 use.[35,36]

Ex vivo regional gene therapy using a LV containing the cDNA for BMP-2 is a promising strategy that allows for sustained release of BMP-2 over several months, thus offering an advantage over recombinant proteins.[29] Prior studies from our lab have used traditionally fabricated demineralized bone matrix, collagen sponge, and ceramic composites as scaffolds to deliver transduced cells to critical-sized bone defects.[19,21,37] In this study we evaluated the ability of the 3D printed HB scaffold to serve as a viable carrier for human ADSCs transduced to overexpress BMP-2.

The HB scaffold is a new, synthetic, osteoregenerative biomaterial which is composed of 90% hydroxyapatite, yet is mechanically elastic which allows it to withstand various deforming forces while being able to retain its innate structure after unloading.[22] It can be printed with mechanical and structural properties that near the load-bearing capacity of human cortical bone.[22,38] Furthermore, it can be readily printed orders of magnitude faster than other 3D-printed scaffolds and avoids the technical and manufacturing limitations of many current scaffolds.[22] Last, it can be printed to precisely fit complex osseous defects on an individual patient basis and its material properties allow for easy intraoperative modification if needed.

Our *in vitro* results demonstrated biocompatibility of the scaffold with transduced human ADSCs, as BMP-2 production was similar between the HB scaffold and control group at 24-h post-transduction. BMP-2 production began to plateau at 7 days post-transduction and was significantly lower than the control group at this time point. This was likely due to greater cell growth in the control group as the 15-mm 3D printed HB disc limited cell expansion due to its small size. Radiographs, histology and histomorphometry all confirmed robust bone formation when the HB scaffold was loaded with transduced human ADSCs and inserted into a mouse muscle pouch. No definite bone formation was noted in the negative control groups.

Although this study demonstrates promising results regarding the combination of 3D printed scaffolds with regional gene therapy for bone repair, there are limitations. First, we only assessed the biocompatibility of the HB scaffold with transduced human ADSCs. We chose to evaluate human ADSCs because they have demonstrated translational promise in regenerative medicine, are an abundant source of mesenchymal stem cells, and are easily harvested with low donor-site morbidity.[39] Second, with regards to our *in vivo* assessment of bone formation, we did not use μ-computed tomography. The HB scaffold is radiopaque; therefore we were unable to identify any bone that may have formed within the scaffold itself in the negative control groups. However, our cross-sectional histological images did not demonstrate bone formation in the negative control groups. Last, we assessed bone formation in a mouse muscle pouch. The translational potential of this strategy needs to be assessed in a more rigorous model such as a critical-sized femoral bone defect.

To the authors' knowledge, this is the first study demonstrating the biocompatibility of a highly osteoconductive 3D printed scaffold combined with a prolonged osteoinductive signal achieved through *ex vivo* regional gene therapy by transducing human ADSCs to overexpress BMP-2. The 3D printed HB scaffold has promising translatable clinical potential because it can be designed to precisely fit skeletal defects on an individual patient basis, is readily malleable yet retains biomechanical properties similar to that of cortical bone, and also supports the delivery of transduced human cells that overexpress a highly osteoinductive signal. Further studies in more rigorous models are needed to further evaluate this novel approach to bone regeneration.

Supplementary Material

Refer to Web version on PubMed Central for supplementary material.

ACKNOWLEDGMENTS

Cannon lab (Keck School of Medicine, Department of Molecular Microbiology & Immunology), Evan Lopez, Dr Robert Yoho.

Contract grant sponsor: National Institutes of Health; contract grant number: R01AR057076

Contract grant sponsor: Eli and Edythe Broad Foundation (RA)

Contract grant sponsor: Google Gift (RNS)

Contract grant sponsor: The Hartwell Foundation (AEJ)

REFERENCES

1. Verettas DA, Galanis B, Kazakos K, Hatziyiannakis A, Kotsios E. Fractures of the proximal part of the femur in patients under 50 years of age. Injury 2002;33:41–45. [PubMed: 11879831]
2. Bucholz RW. Nonallograft osteoconductive bone graft substitutes. Clin Orthop Relat Res 2002;395:44–52.
3. Mastrogiacomo M, Muraglia A, Komlev V, Peyrin F, Rustichelli F, Crovace AC, Cancedda R. Tissue engineering of bone: search for a better scaffold. Orthod Craniofac Res 2005;8:277–284. [PubMed: 16238608]
4. Younger EM, Chapman MW. Morbidity at bone graft donor sites. J Orthop Trauma 1989;3:192–195. [PubMed: 2809818]
5. Ahlmann E, Patzakis M, Roidis N, Shepherd L, Holtom P. Comparison of anterior and posterior iliac crest bone grafts in terms of harvest-site morbidity and functional outcomes. J Bone Joint Surg Am 2002;84-A:716–720. [PubMed: 12004011]
6. Dell PC, Burchardt H, Glowczewskie FP. A roentgenographic, bio-mechanical, and histological evaluation of vascularized and non-vascularized segmental fibular canine autografts. J Bone Joint Surg Am 1985;67:105–112. [PubMed: 3881445]
7. Alaee F, Virk MS, Tang H, Sugiyama O, Adams DJ, Stolina M, Dwyer D, Ominsky MS, Ke HZ, Lieberman JR. Evaluation of the effects of systemic treatment with a sclerostin neutralizing antibody on bone repair in a rat femoral defect model. J Orthop Res 2014;32:197–203. [PubMed: 24600701]
8. Jeon O, Song SJ, Kang SW, Putnam AJ, Kim BS. Enhancement of ectopic bone formation by bone morphogenetic protein-2 released from a heparin-conjugated poly(L-lactic-co-glycolic acid) scaffold. Biomaterials 2007;28:2763–2771. [PubMed: 17350678]

9. Lin ZY, Duan ZX, Guo XD, Li JF, Lu HW, Zheng QX, Quan DP, Yang SH. Bone induction by biomimetic PLGA-(PEG-ASP)n copolymer loaded with a novel synthetic BMP-2-related peptide in vitro and in vivo. J Control Release 2010;144:190–195. [PubMed: 20184932]
10. Chan DS, Garland J, Infante A, Sanders RW, Sagi HC. Wound Complications Associated with BMP-2 in Orthopaedic Trauma Surgery. J Orthop Trauma 2014;28:599–604. [PubMed: 24682163]
11. Carragee EJ, Hurwitz EL, Weiner BK. A critical review of recombinant human bone morphogenetic protein-2 trials in spinal surgery: emerging safety concerns and lessons learned. Spine J 2011;11:471–491. [PubMed: 21729796]
12. Warnke PH, Seitz H, Warnke F, Becker ST, Sivananthan S, Sherry E, Liu Q, Wiltfang J, Douglas T. Ceramic scaffolds produced by computer-assisted 3D printing and sintering: characterization and biocompatibility investigations. J Biomed Mater Res B Appl Bio- mater 2010;9999B: 212–217.
13. Sanz-Herrera JA, Doblaré M, García-Aznar JM. Scaffold micro-architecture determines internal bone directional growth structure: a numerical study. J Biomech 2010;43:2480–2486. [PubMed: 20542275]
14. Wang H, Wu G, Zhang J, Zhou K, Yin B, Su X, Qiu G, Yang G, Zhang X, Zhou G, Wu Z. Osteogenic effect of controlled released rhBMP-2 in 3D printed porous hydroxyapatite scaffold. Colloids Surfaces B Biointerfaces 2016;141:491–498. [PubMed: 26896655]
15. Temple JP, Hutton DL, Hung BP, Huri PY, Cook CA, Kondragunta R, Jia X, Grayson WL. Engineering anatomically shaped vascularized bone grafts with hASCs and 3D-printed PCL scaffolds. J Biomed Mater Res A 2014;102:4317–4325. [PubMed: 24510413]
16. Roskies M, Jordan JO, Fang D, Abdallah MN, Hier MP, Mlynarek A, Tamimi F, Tran SD. Improving PEEK bioactivity for craniofacial reconstruction using a 3D printed scaffold embedded with mesenchymal stem cells. J Biomater Appl 2016; 31:132–139. [PubMed: 26980549]
17. Lee MK, Deconde AS, Lee M, Walthers CM, Sepahdari AR, Elashoff D, Grogan T, Bezouglaia O, Tetradis S, St John M, Aghaloo T. Biomimetic scaffolds facilitate healing of critical-sized segmental mandibular defects. Am J Otolaryngol 2015;36:1–6. [PubMed: 25109658]
18. Shim J-H, Kim SE, Park JY, Kundu J, Kim SW, Kang SS, Cho DW. Three-dimensional printing of rhBMP-2-loaded scaffolds with long-term delivery for enhanced bone regeneration in a rabbit diaphyseal defect. Tissue Eng Part A 2014;20:1980–1992. [PubMed: 24517081]
19. Lieberman JR, Daluiski A, Stevenson S, Wu L, McAllister P, Lee YP, Kabo JM, Finerman GA, Berk AJ, Witte ON. The effect of regional gene therapy with bone morphogenetic protein-2-producing bone-marrow cells on the repair of segmental femoral defects in rats. J Bone Joint Surg Am 1999;81:905–917. [PubMed: 10428121]
20. Hsu WK, Sugiyama O, Park SH, Conduah A, Feeley BT, Liu NQ, Krenek L, Virk MS, An DS, Chen IS, Lieberman JR. Lentiviral-mediated BMP-2 gene transfer enhances healing of segmental femoral defects in rats. Bone 2007;40:931–938. [PubMed: 17236835]
21. Virk MS, Sugiyama O, Park SH, Gambhir SS, Adams DJ, Drissi H, Lieberman JR. “Same day” ex-vivo regional gene therapy: a novel strategy to enhance bone repair. Mol Ther 2011;19:960–968. [PubMed: 21343916]
22. Jakus AE, Rutz AL, Jordan SW, Kannan A, Mitchell SM, Yun C, Koube KD, Yoo SC, Whiteley HE, Richter CP, Galiano RD, Hsu WK, Stock SR, Hsu EL, Shah RN. Hyperelastic “bone”: A highly versatile, growth factor–free, osteoregenerative, scalable, and surgically friendly biomaterial. Sci Transl Med 2016;8:358ra127.
23. Jakus AE, Shah RN. Multi and mixed 3D-printing of graphene-hydroxyapatite hybrid materials for complex tissue engineering. J Biomed Mater Res A 2017;105:274–283. [PubMed: 26860782]
24. Jakus AE, Koube KD, Geisendorfer NR, Shah RN. Robust and elastic lunar and martian structures from 3D-printed regolith inks. Sci Rep 2017;(7:):44931.
25. Jakus AE, Taylor SL, Geisendorfer NR, Dunand DC, Shah RN. Metallic Architectures from 3D-Printed Powder-Based Liquid Inks. Adv Fucntional Mater 2015;25:6985–6995.
26. Taylor SL, Jakus AE, Shah RN, Dunand DC. Iron and Nickel Cellular Structures by Sintering of 3D-Printed Oxide or Metallic Particle Inks. Adv Eng Mater 2016;
27. Jakus AE, Secor EB, Rutz AL, Jordan SW, Hersam MC, Shah RN. Three-Dimensional Printing of High-Content Graphene Sca ff olds for Electronic and Biomedical Applications. ACS Nano 2015;9: 4636–4648. [PubMed: 25858670]

28. Zuk PA, Zhu M, Mizuno H, Huang J, Futrell JW, Katz AJ, Benhaim P, Lorenz HP, Hedrick MH. Multilineage cells from human adipose tissue: implications for cellbased therapies. Tissue. Eng 2001;7: 211–228. [PubMed: 11304456]
29. Sugiyama O, Sung An D, Kung SP, Feeley BT, Gamradt S, Liu S, Liu NQ, Chen IS, Lieberman JR. Lentivirus-mediated gene transfer induces long-term transgene expression of BMP-2 In vitro and new bone formation in vivo. Mol Ther 2005;11:390–398. [PubMed: 15727935]
30. Will J, Melcher R, Treul C, Travitzky N, Kneser U, Polykandriotis E, Horch R, Greil P. Porous ceramic bone scaffolds for vascularized bone tissue regeneration. J Mater Sci Mater Med 2008;19: 2781–2790. [PubMed: 18305907]
31. Inzana JA, Olvera D, Fuller SM, Kelly JP, Graeve OA, Schwarz EM, Kates SL, Awad HA. 3D printing of composite calcium phosphate and collagen scaffolds for bone regeneration. Biomaterials 2014;35:4026–4034. [PubMed: 24529628]
32. Ishack S, Mediero A, Wilder T, Ricci JL, Cronstein BN. Bone regeneration in critical bone defects using three-dimensionally printed β-tricalcium phosphate/hydroxyapatite scaffolds is enhanced by coating scaffolds with either dipyridamole or BMP-2. J Biomed Mater Res B Appl Biomater 2015;102:366–375.
33. Wilson CE, de Bruijn JD, van Blitterswijk CA, Verbout AJ, Dhert WJ. Design and fabrication of standardized hydroxyapatite scaffolds with a defined macro-architecture by rapid prototyping for bone-tissue-engineering research. J Biomed Mater Res A 2004;68: 123–132. [PubMed: 14661257]
34. Alaee F, Hong SH, Dukas AG, Pensak MJ, Rowe DW, Lieberman JR. Evaluation of osteogenic cell differentiation in response to bone morphogenetic protein or demineralized bone matrix in a critical sized defect model using GFP reporter mice. J Orthop Res 2014;32:1120–1128. [PubMed: 24888702]
35. Brannan PS, Gaston RG, Loeffler BJ, Lewis DR. Complications With the Use of BMP-2 in Scaphoid Nonunion Surgery. J Hand Surg Am 2016;41:602–608. [PubMed: 27013317]
36. Chrastil J, Low JB, Whang PG, Patel AA. Complications associated with the use of the recombinant human bone morphogenetic proteins for posterior interbody fusions of the lumbar spine. Spine (Phila Pa 1976) 2013;38:E1020–E1027.
37. Wang JC, Kanim LE, Yoo S, Campbell PA, Berk AJ, Lieberman JR. Effect of regional gene therapy with bone morphogenetic protein- 2-producing bone marrow cells on spinal fusion in rats. J Bone Joint Surg Am 2003;85-A:905–911. [PubMed: 12728043]
38. Zioupos P, Currey JD. Changes in the stiffness, strength, and toughness of human cortical bone with age. Bone 1998;22:57–66. [PubMed: 9437514]
39. Hicok KC, Du Laney TV, Zhou YS, Halvorsen YD, Hitt DC, Cooper LF, Gimble JM. Human adipose-derived adult stem cells produce osteoid in vivo. Tissue Eng 2004;10:371–380. [PubMed: 15165454]

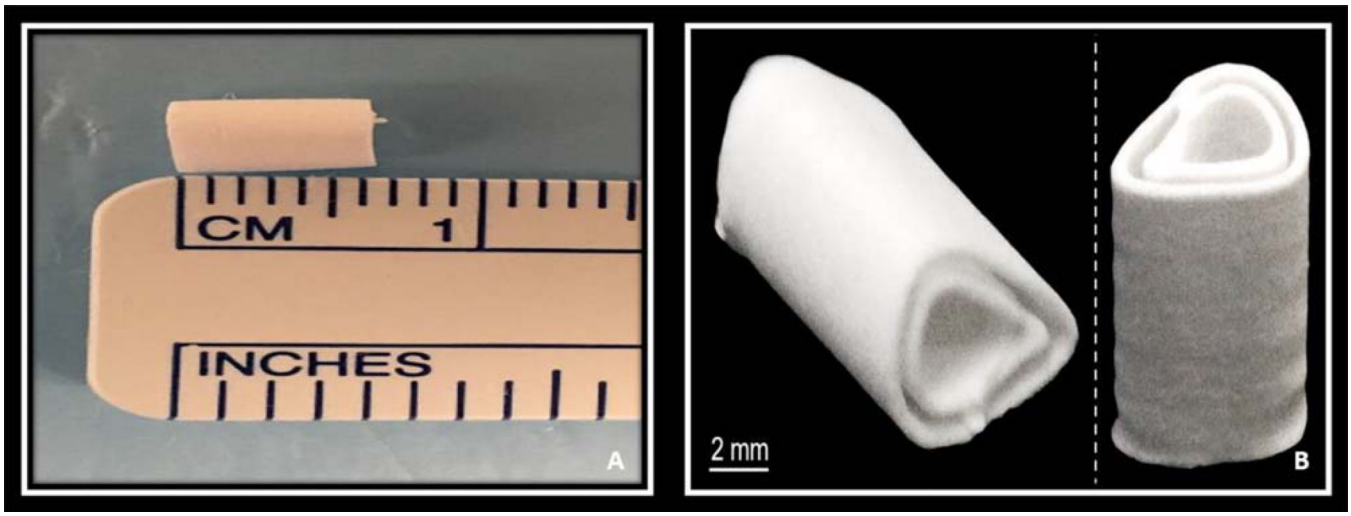

FIGURE 1.

A: Image of the HB 3D printed scaffold after completion of the fabrication process. B: Cross-sectional image demonstrating the high porosity of the scaffold with open channels at each end to facilitate vascular ingrowth and bone formation.

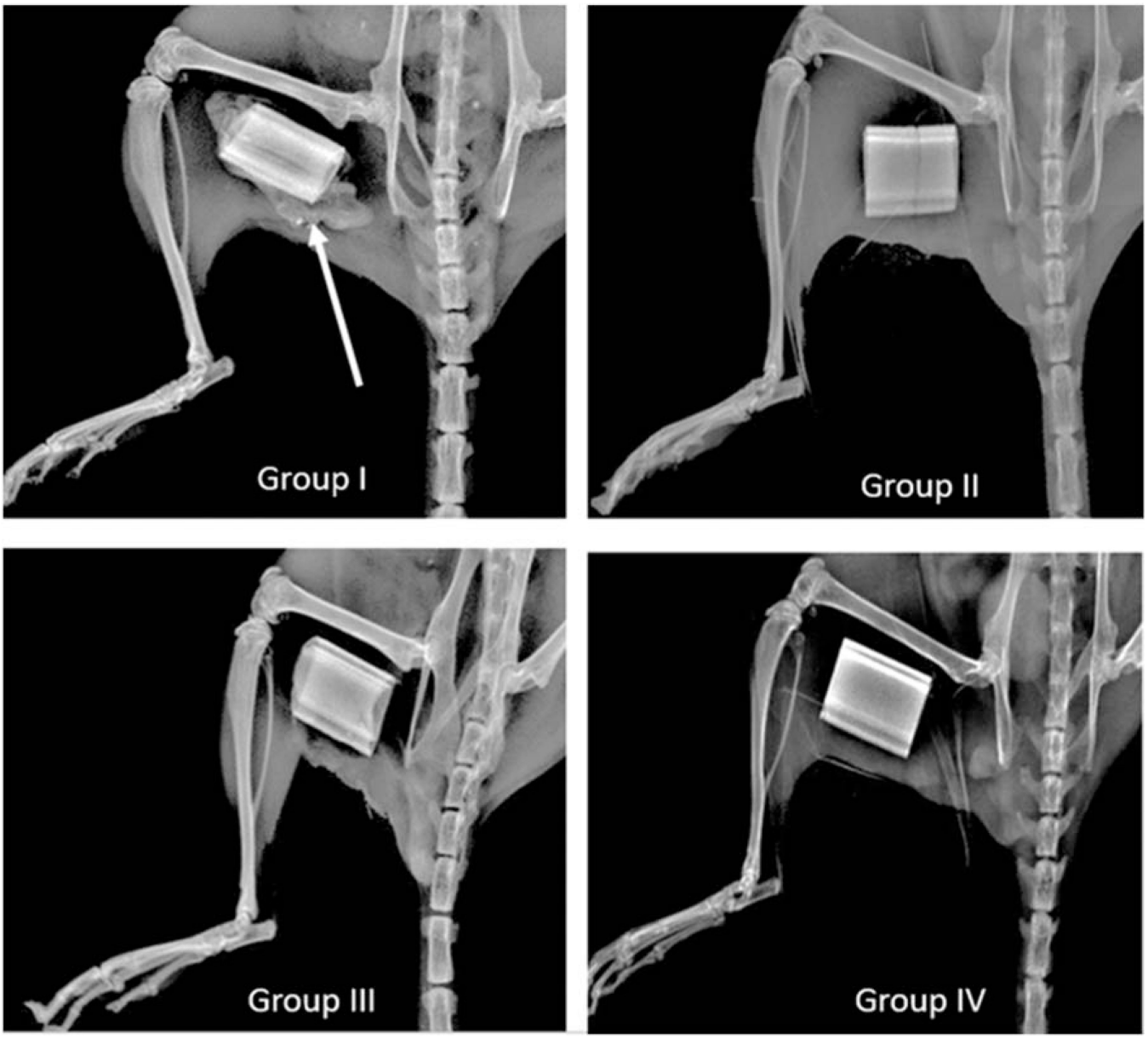

FIGURE 2.

Plain radiographs taken at 2 weeks after implantation of ADSCs on the HB scaffold or HB scaffold alone in a hind limb muscle pouch. There is evidence of robust bone formation (white arrow) in the group implanted with ADSCs transduced with a LV carrying the cDNA for BMP-2 (group I, top left). There is no evidence of bone formation in groups II–IV (group II- ADSC/LV-GFP 1 HB Scaffold, group III- Nontransduced ADSC + HB Scaffold, group IV–HB Scaffold Alone).

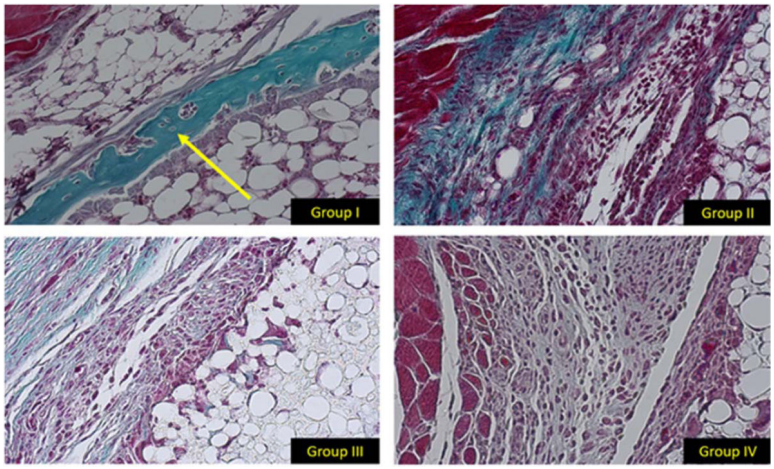

FIGURE 3.

20× histology images stained with MT. The histological slices represent the same area of each muscle pouch at the interface between the exterior of the HB scaffold and native muscle. In group I there is evidence of woven bone formation (yellow arrow). There is no evidence of bone formation in groups II–IV.

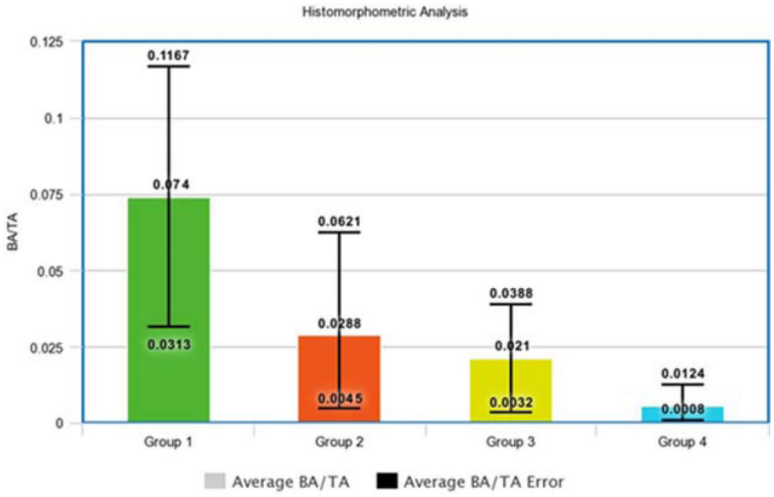

FIGURE 4.

Histomorphometry calculations of average BA to TA ratios between the four animal groups. The error bars represent the upper and lower limits of the BA/TA ratio among the five animals in each group. The BA/TA ratio was significantly greater in group I compared with groups II–IV ($p = 0.002$). (group I- ADSC/LV-BMP-2 + HB Scaffold, group II- ADSC/LV-GFP + HB Scaffold, group III- Nontransduced ADSC + HB Scaffold, group IV- HB Scaffold Alone).

TABLE I.

In vivo Animal Study Groups

Group	*n*	Treatment
I (experimental)	5	ADSC/LV-BMP-2 + HB Scaffold
II (negative control)	5	ADSC/LV-GFP + HB Scaffold
III (negative control)	5	Nontransduced ADSC + HB Scaffold
IV (negative control)	5	HB Scaffold Alone

TABLE II.

ELISA of BMP-2 Production at 24 h, 1, and 2 Weeks After Transduction of Human ADSCs With a LV Vector Containing the cDNA for BMP-2

	BMP2 production (ng/24 h/1 X 10^6 cells)		
Time Point	**Human ADSC/ LV-BMP2**	**Human ADSC/ LV-BMP2 1 HB Scaffold**	***p*-value**
24 h	20.4 ± 0.62	21.1 ± 2.32	0.651
1 week	365 ± 15.2	61.7 ± 35.6	<0.001
2 weeks	1015 ± 54.0	76.3 ± 34.0	<0.001

Human ADSC/LV-BMP2 were loaded in an empty well (cells alone) to serve as a control group. The experimental group consisted of human ADSC/LV-BMP-2 loaded on a 3D printed HB 15-mm disc.